23rd International Conference on Material Forming (ESAFORM 2020)

# Integrated Design in Welding and Incremental Forming: Material Model Calibration for Friction Stir Welded Blanks

António Andrade-Campos[a,*], Sandrine Thuillier[b], João Martins[a,b], Pierpaolo Carlone[c], Fausto Tucci[c], Robertt Valente[a], Rui M. F. Paulo[d] and Ricardo J. Alves de Sousa[a]

[a]*Center for Mechanical Technology and Automation, Dep. Mechanical Engineering, University of Aveiro,Portugal*
[b]*Univ. Bretagne Sud, UMR CNRS 6027, IRDL, F-56100 Lorient, France*
[c]*Department of Industrial Engineering, University of Salerno, Via Giovanni Paolo II, 132, Fisciano (SA), Italy*
[d]*School of Mechanical and Aerospace, Queen's University Belfast, United Kingdom*

* Corresponding author. Tel.: +351-234-380-830 ; fax: +350-234-380-953. *E-mail address:* gilac@ua.pt

**Abstract**

Typically, the development of new forming products is performed using numerical tools such as finite element analysis software. However, the precision of these tools is dependent on the input data, particularly the one related to constitutive models and material parameters. These parameters are generally used to calibrate the model for each specific material, knowing *a priori* that the material behavior and properties are constant within the part/specimen. However, in welded blanks, the material behavior and properties drastically change with the proximity to the welded zone and, therefore, new challenges arise with the calibration of constitutive models for such heterogenous materials. The present study is part of a larger project that deals with the incremental forming of welded aluminum blanks. These are initially joined by Friction Stir Welding (FSW), and tensile tests were carried out both on the base material and on the welded material, transversely to the weld, using a Digital Image Correlation (DIC) device to capture the strain field. Moreover, hardness measurements were carried out. Results show the evolution of change on the material behavior and properties throughout three well distinct areas, namely: the nugget zone at the center of the weld; the thermo-mechanically affected zone (TMAZ); and the heat affected zone (HAZ), making it possible to create a suitable elastoplastic model with multi-linear piecewise function parameters, properly calibrated for the friction stir welded material. A finite element model updating scheme was applied using a smooth interpolation scheme for the DIC data with outliers and gap control. The calibration process resulted in a model with quite good accuracy in comparison to experimental results.

*Keywords:* Integrated design; welding; FSW; model calibration; parameter identification; finite element model updating.

## 1. Introduction

Sheet metal parts are developed and required for a large number of industries, such as transportation, food, health, among others [1]. Generally, the manufacturing process of sheet metal parts is a multi-stage procedure involving forming, cutting, assembly and, often, joining by welding. The efficiency of this multi-stage process can still be increased with the simultaneously integration/combination of some technological processes. However, research in metal forming is generally focused in the development of a single process and not in the integration of several of them. The work presented here is a task of a more comprehensive project whose aim is to combine Friction Stir Welding (FSW) and Single Point Incremental Forming (SPIF) technologies, for reliable and structurally-optimized components. The integration of these processes can contribute to material savings and to the decrease of some operations, such as cutting. To demonstrate the effective feasibility of the SPIF process on FSW sheets, several tasks must be performed, as illustrated in Fig. 1.
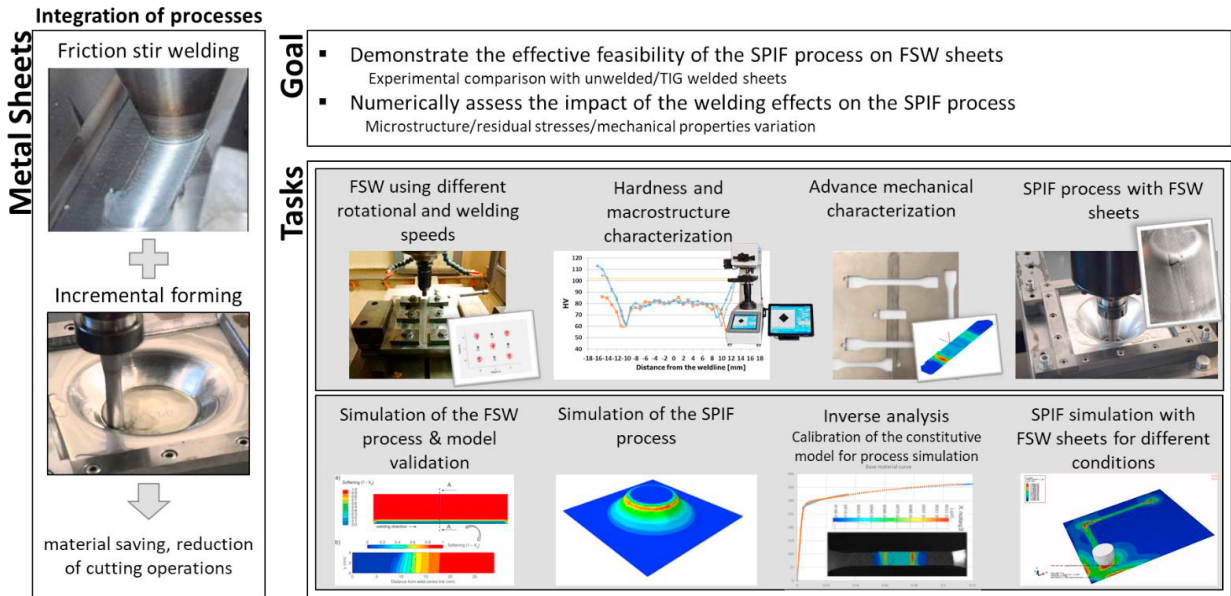
Fig. 1. Framework of the study presented here and its goals. The integration of FSW and SPIF can lead to material savings and reduction of some mechanical technological operations.

Typically, numerical simulation is used to design sheet metal structures. However, in the simulation field as well, the majority of the analysis are made for each specific step. Therefore, there is a huge interest to simulate the whole process, instead of focusing on some of the most important stages, in order to improve the reliability of the numerical predictions. Nevertheless, such an integrated design of the whole manufacturing process is a complex route, and experimental validation is still necessary [1]. Consequently, the global project also includes numerical analyses of an integrated process dealing with the forming of welded aluminium blanks. In particular, it aims to numerically assess the impact of the welding effects on the SPIF process. For this goal, several numerical tasks, also listed in Fig. 1, are required for the integrated project.

In order for the simulation to contribute positively to the design and analysis of metal forming processes, the constitutive model used must be accurate. Otherwise, the results achieved may not reproduce the real behavior of the material and/or of the process. The accuracy of the constitutive model is directly related to the mathematical formulation and to the calibration. Complex formulations lead to the reproduction of a large number of phenomena, however, also require both high CPU effort in simulations and hard work to be calibrated. Generally, these formulations include more than a dozen of parameters to be identified for each material. Therefore, the industrial approach relies on the use of non-sophisticated models that run easily in Finite Element Analysis (FEA) software packages, and depend on only 3 to 6 parameters to be identified.

There are several successful Full-Field Methodologies (FFM) to calibrate non-linear elastoplastic constitutive models. These methodologies can be classified in external and balance methods. The firsts use the experimental observations/data as a reference to the numerical model. Therefore, these methods search the parameters that lead the numerical simulations (using

the model) towards the experimental data, without mixing the experimental data with the numerical one. A scheme of an external method, particularly the Finite Element Model Updating (FEMU) method, can be seen in Fig. 2. These methods are easy to implement, but require that the boundary conditions of the numerical simulation reproduce with accuracy the conditions of the experimental apparatus. Balance methods, such as the Virtual Field Method (VFM) [2], directly use the local experimental data (e.g. displacements or strains obtained by DIC) as input and the constitutive model to calculate the internal work. The parameters are searched using the deviation between the internal and the external work (using the experimental external loads) as criterion to be minimized. The advantages of the balance methods are their stability and not requiring boundary conditions, however, generally they use some kind of sophisticated physical or mathematical technique to filter the solutions. For the VFM, the principle of virtual work is used, and, consequently, the selected virtual fields work as filters.
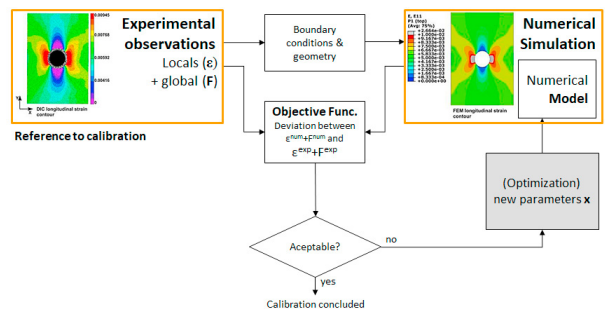


Fig. 2. Parameter identification procedure using the Finite Element Model Updating (FEMU) method.

In this work, a FEMU methodology is applied to calibrate an AA6082-T6 subjected to FSW. It is known (as shown in [1,2]) that properties of a welded material change spatially, becoming a locally-heterogeneous material. In welded blanks, the material behavior and properties change with the proximity to the welded zone. Therefore, an elastoplastic model with multi-linear piecewise function parameters is calibrated for a friction stir welded material using tensile tests and a DIC technique.

**Nomenclature**

| | |
|---|---|
| $F$ | force of the load cell |
| $\varepsilon$ | strain |
| $n_p$ | number of measuring points |
| $n_s$ | number of timesteps |
| $a, b$ | coefficients of the linear function that defines the parameters |
| $y$ | distance to the welding nugget centre |
| $f_{FEMU}$ | objective function for the FEMU method |

## 2. Experimental results

As detailed in [1], AA6082-T6, provided in rolled sheets of thickness 2 mm, was joined by FSW in squared welded samples of side dimension 220 mm. The weld line is parallel to the rolling direction. FSW is performed using the following conditions: *Rotational speed / Feed rate* = (A) 1000 rpm / 40 mm.min$^{-1}$ and (C) 1200 rpm / 70 mm.min$^{-1}$. The mechanical behavior of both the base material and the weld is characterized in tension. Samples are cut through the welding line, so that the welded area lies in the specimen center. A sample dimension of gauge length of 68 mm and a width of 10 mm is used, for samples cut along the rolling direction. Tensile tests are performed with an Instron machine of maximum capacity 50 kN and a corresponding load cell. The average strain rate is equal to $1 \times 10^{-3} s^{-1}$, calculated using DIC within the area corresponding to the tool shoulder diameter (average value over a rectangular area of length 12 mm and width equal to the sample width, located in the center of the gauge area).

Results of tensile tests on the base material and on welded samples are presented in Fig. 3. It can be seen that the average stress is significantly lower for the welded specimen, whatever the parameters of the FSW process. The initial yield stress is roughly divided by two, which is consistent with the hardness measures (Fig. 4). For more details concerning the experimental data, see [1]. The crosshead displacement of test A is used as boundary condition for the numerical tests.

## 3. Material model and methodology

The constitutive model used in this work is the von Mises yield criterion with isotropic hardening. Note that the use of a simple model does not constraint the generality of the methodology used. The yield surface in plasticity can be written as

$$f = \bar{\sigma}(\boldsymbol{\sigma}) - \sigma_Y(\bar{\varepsilon}^p) = 0 , \qquad (1)$$

where $\bar{\sigma}(\boldsymbol{\sigma})$ is the von Mises equivalent stress and $\sigma_Y(\bar{\varepsilon}^p)$ is the flow stress.
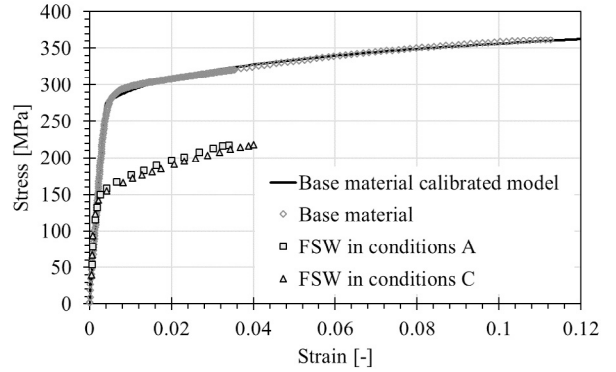


Fig. 3. Stress-strain curves for the base material in TD and for the FSW samples in different conditions (rotational speed/Feed rate = 1000 rpm/ 40 mm. min$^{-1}$ for A and 1200 rpm/ 70 mm.min$^{-1}$ for C). Stress-strain curve of the base material model calibrated using a curve-fitting method.
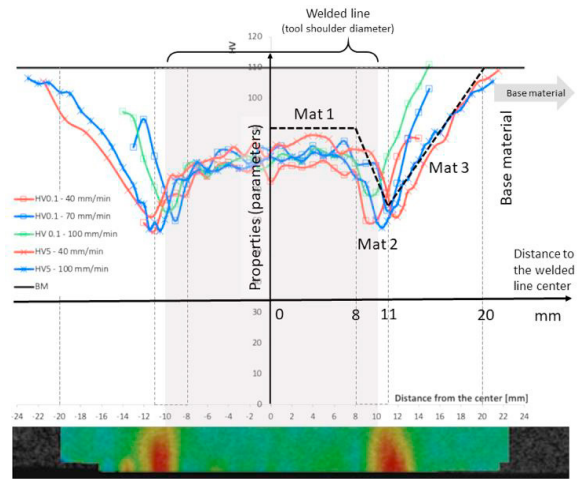


Fig. 4. Micro- and macro-hardness measurements across the FS weld (rotational speed = 1000 rpm). Below, strain distribution recorded by DIC. It is supposed that the hardening properties and, consequently, the parameters, change linearly.

The evolution of the flow stress is defined by the phenomenological Swift's law, mathematically defined by

$$\sigma_Y(\bar{\varepsilon}^p) = k(\varepsilon_0 + \bar{\varepsilon}^p)^n, with \ \varepsilon_0 = \left(\frac{\sigma_0}{k}\right)^{\frac{1}{n}}. \qquad (2)$$

$\mathbf{x} = (\sigma_0, n, k)$ is the material parameter set, which is used to calibrate the constitutive model.

Results from the hardness measurements showed that the FSW material behavior and properties change throughout three well distinct areas, such as the nugget zone at the center of the weld (Mat 1), the thermo-mechanically affected zone (Mat 2) and the heat affected zone (Mat 3), as illustrated in Fig. 4. It is expected that the hardening of the material also changes correspondingly. Therefore, using the above presented elastoplastic model,

multi-linear piecewise function parameters were used to capture the material behavior that evolves with the distance to the weld center.

Considering that it is necessary to impose continuity conditions between the different regions, the parameter $x_{i,j}$, with $i = 2, ..., n_{MAT}$ and $j = 1, ..., n_{parameters}$ can be mathematically defined as

$$x_{i,j} = a_{i,j}y + b_{i,j}, \qquad (3)$$

where $y$ is the distance to the welding center and

$$a_{i,j} = \frac{x_{i,j} - x_{i-1,j}}{y_i - y_{i-1}}, \qquad (4)$$

$$b_{i,j} = x_{i-1,j} - y_{i-1}a_{i,j}. \qquad (5)$$

In this work, $x_{i,1} = \sigma_0$, $x_{i,2} = n$ and $x_{i,3} = k$. The previous equations change each parameter, as illustrated in Fig. 4, when the distance $y$ equals the characteristics values of $y_1 = 8$, $y_2 = 11$ and $y_3 = 20$ mm. For Mat 1, the parameters are constant. For Mat 2 and Mat 3, these parameters change linearly using their values for distance $y_1$, $y_2$ and $y_3$ as reference. However, considering that the properties and, consequently, the parameters for $y > y_3$ are the ones of the base material, only the parameters in $y_1$, $y_2$ must be identified, representing 6 parameters, i.e. $\mathbf{x} = (x_1, x_2, x_3, x_4, x_5, x_6)$ or, specifically $\mathbf{x} = (\sigma_{0,y_1}, n_{y_1}, k_{y_1}, \sigma_{0,y_2}, n_{y_2}, k_{y_2})$ to be identified. It is worth noticing that, in this work, the welding direction is not considered, resulting in symmetry of properties (symmetry of the left and right side of Fig. 4). If this symmetry had not been considered, only an extra set of parameters would have been necessary (adding only a Mat 4 material). Although the parameters only change linearly in each region, it results in an even more non-linear hardening behavior than the original constitutive model. This model is implemented in the finite element commercial code ABAQUS® by means of a user material (UMAT) subroutine.

The constitutive model calibration methodology used in this work is the FEMU methodology, generally described in Fig. 2. The local experimental observations are the in-plane strain field recorded by the ARAMIS system, from GOM, and the global observations are the loads measured by the load cells of the standard tensile machine. The objective function considers both experimental observations in a normalized formulation that gives the same weight for each contribution:

$$f_{FEMU}(\mathbf{x}) = \frac{1}{n_s}\sum_{i=1}^{n_s}\{f_{local}(\mathbf{x}) + f_{global}(\mathbf{x})\}, \qquad (6)$$

where

$$f_{local}(\mathbf{x}) = \frac{1}{n_p}\sum_{j=1}^{n_p}\left[\sum_{l=xx,yy,xy}\left(\frac{\varepsilon_{i,j,l}^{num}(\mathbf{x}) - \varepsilon_{i,j,l}^{exp}}{\varepsilon_{i,j,l}^{exp}}\right)^2\right], \text{ and} \qquad (7)$$

$$f_{global}(\mathbf{x}) = \left(\frac{F_i^{num}(\mathbf{x}) - F_i^{exp}}{F_i^{exp}}\right)^2. \qquad (8)$$

Considering that the objective function of equations 6-8 presents a least-square structure, the Levenberg-Marquardt optimization method [4] was applied using a finite differences technique to calculate the Jacobian matrix.

## 4. Identification of the base material

For the base material, a non-linear curve-fitting method was used with the Generalized Reduce Gradient (GRG) optimization method [4]. The tensile stress-strain curve of the calibrated model, which can be seen in Fig. 3, reproduces quite well the tensile behavior of the AA6082-T6 base material. The parameters found are $\mathbf{x}_{base\ mat} = (\sigma_0 = 274.83$ MPa, $n = 0.094$, $k = 441.69$ MPa).

## 5. Experimental *vs* numerical local data

The FEMU methodology requires a direct local comparison of the experimental data with the numerical one. However, generally, the experimental data is achieved using Full-field methods in points with space localization rather different from the numerical nodes or integration points. Therefore, an interpolation scheme must be used to compare the experimental data with the numerical one, at the same points. Although interpolation procedures seem to be straightforward, different methods can be applied and such a selection must be done carefully, as it has a large impact on the results. For this work, a cubic-spline interpolation method was used in opposition to the linear, nearest neighbor, cubic hermite and biharmonic methods [3]. Although the methodology used allows extrapolation to external points, it was decided not to use this option. Additionally, experimental measured points were filtered, neglecting possible outliers and absence of data (gaps due to DIC technique). These points were not considered when calculating equation 6. Fig. 5 illustrates both the space localization of the experimental and numerical points and an example of interpolation of the strain field.

## 6. Identification of the welded material: results

The identification process took 682 evaluations of $f_{FEMU}(\mathbf{x})$ defined by equation 6 to converge to the parameters listed in Table 1. The stress-strain curve obtained using the global force and displacement of the specimen can be seen in Fig. 6. This curve reproduces very well the global behavior of the FSW specimen and demonstrates that the error of $f_{global}$ (equation 8) is low. In fact, the final value for the objective function obtained is 0.0483 (5% of the initial value), as can be seen in Fig. 7. The figure also shows the evolution of each parameter during the optimization process, demonstrating convergence of the identification process.

Fig. 8 represents the distribution of the parameters as a multi-linear piecewise function of the distance to the welding center. It can be seen that, although parameter $\sigma_0$ decreases in the thermo-mechanical affected zone (similarly to the micro-hardness tests), parameter $n$ increases to the TMAZ-HAZ boundary and decreases up to the base material. Parameter $k$ does not change the slope during the space distribution, increasing the value up to the base material.

Figures 9 and 10 show the strain distribution for the experimental test, recorded with the DIC system, and for the numerical tensile test for different times. From Fig. 9, the general strain gradients seem to be well captured by the numerical model. However, from Fig.10, it can be noticed that, near necking, and consequently rupture, some differences between the experimental and numerical strain field arise.
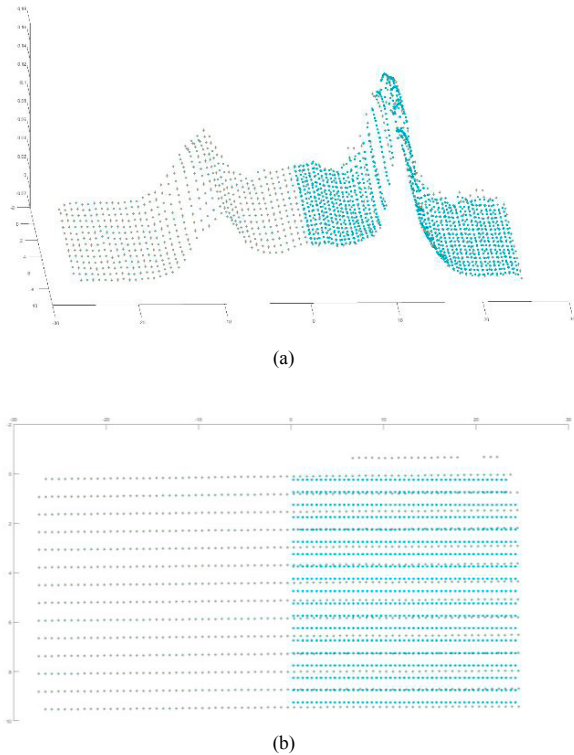


(a)



(b)

Fig. 5. Space interpolation scheme of the experimental data (in green color) to the numerical (light blue color): (a) example of interpolation for the strain field, (b) space localization of the points.
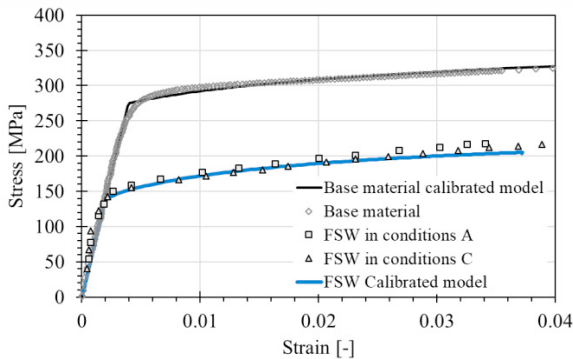


Fig. 6. Comparison of the experimental and numerical stress-strain curves. The stress-strain curves for the FSW (both experimental and numerical with the calibrated model) correspond to the global strain and stress.
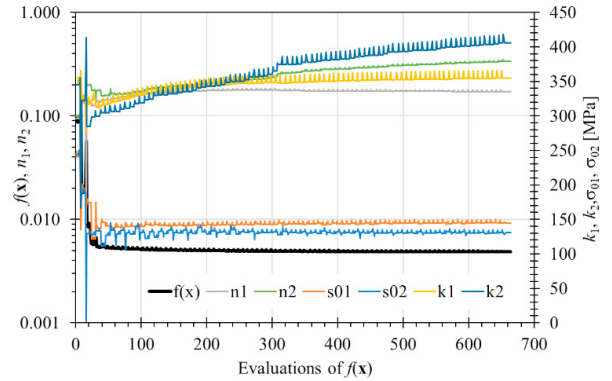


Fig. 7. Evolution of the objective function $f(\mathbf{x})$ with the optimization evaluations. Evolution and convergence of the constitutive parameters in the FEMU process.
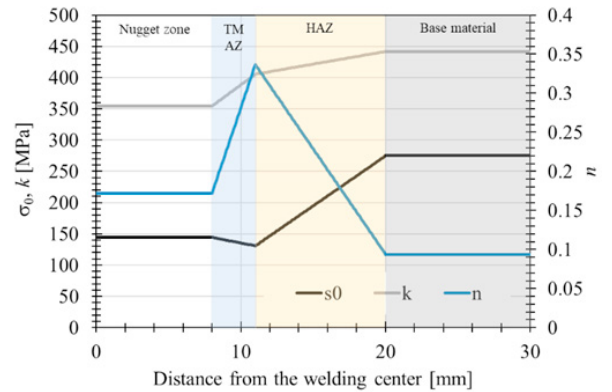


Fig. 8. Multi-linear piecewise function parameters calibrated using a FEMU identification method.

## 7. Conclusion

A FEMU methodology was applied to the hardening characterization of a FSW material, where material behavior and properties change through three well distinct areas (the nugget zone at the center of the weld, the thermo-mechanically affected zone and the heat affected zone). In this work, it was considered that the properties (and, consequently, hardening) continuously and smoothly change though these three zones. Having the hardness measurements as a reference, the nugget zone presents constant properties. However, the values of the properties decrease in the thermo-mechanically affected zone up to the boundary of the heat affected zone, where these values increase up to the base material. Therefore, an isotropic Swift hardening model with multi-linear piecewise function parameters was used to capture this material behavior that change with the distance to the welding center.

The calibration of the numerical model resulted in a constitutive model capable of reproducing quite well the behavior of the FSW AA6082-T6 sheet.

In this work, some simplifications were made. Results of Figure 4, 5 and 10 show that hardening is not symmetric. However, in this work, a symmetric model was adopted.

Nevertheless, the methodology here presented can be straightforward extended for the non-symmetry condition.
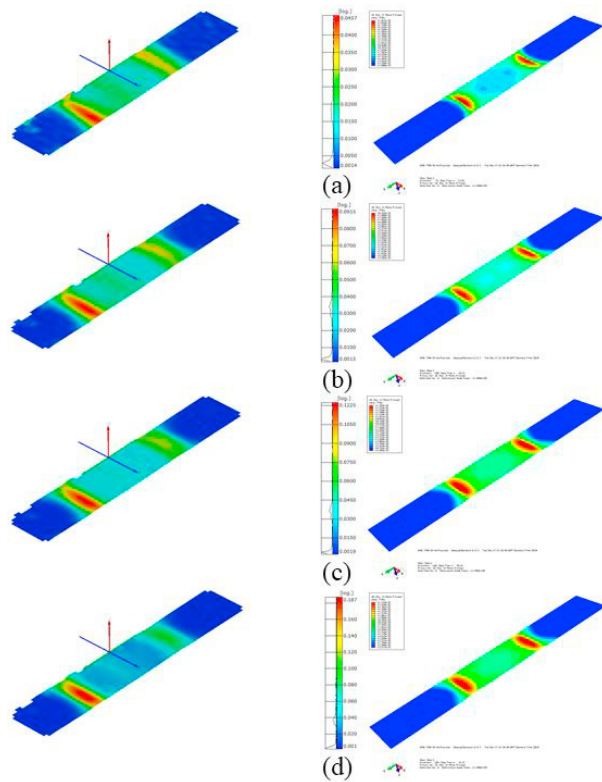


Fig. 9. Principal strain $\varepsilon_1$ distribution at different time steps (experimental at the left and numerical at the right): (a) 12, (b) 19, (c) 29 and (d) 37 s.
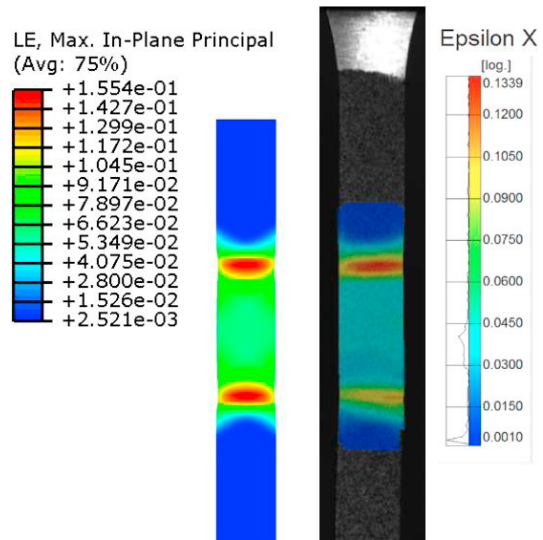


Fig. 10. Strain distribution just before necking (numerical at the left and experimental at the right for the time step of 37 s). The dissymmetry in the sample width recorded in the experiments could be further reproduced using local displacements recorded with DIC as boundary conditions for FEA.

### Acknowledgements

Table 1. Multi-linear piecewise function parameters calibrated for a FSW AA6082-T6.

| Welding Zone | Parameter | Value |
|---|---|---|
| Nugget zone (Mat 1) | $\sigma_0$ [MPa] | 144.38 |
| | $n$ | 0.172 |
| | $k$ [MPa] | 354.44 |
| TMAZ-HAZ boundary | $\sigma_0$ [MPa] | 130.85 |
| | $n$ | 0.337 |
| | $k$ [MPa] | 405.45 |
| Base material | $\sigma_0$ [MPa] | 274.83 |
| | $n$ | 0.094 |
| | $k$ [MPa] | 441.69 |

### References

[1] Thuillier S, Andrade-Campos A, Carlone P, Valente R. and Alves de Sousa R. J, Integrated Design in Welding and Incremental Forming: Mechanical Behavior of Friction Stir Welded Blanks 2019; AIP Conf Proc 2113, 060010; doi: 10.1063/1.5112605.

[2] Le Louëdec G, Pierron F, Sutton M. A, Siviour C, Reynolds A. P, Identification of the Dynamic Properties of Al 5456 FSW Welds Using the Virtual Fields Method, J. Dynamic Behavior Mater. 2015; 1:176–190; doi: 10.1007/s40870-015-0014-6.

[3] Matlab R2019b documentation, Mathworks, 2019.

[4] Nocedal J, Wright S. Numerical Optimization, Springer-Verlag New York. 2006.